Generalized derivation of free-electron-laser harmonic radiation from plane-polarized wigglers

M. J. Schmitt and C. J. Elliott
Los Alamos National Laboratory, Los Alamos, New Mexico 87545
(Received 3 November 1989)

Radiation at the harmonic frequencies in free-electron lasers is affected by several factors including misalignment of the electron beam and wiggler axes, and transverse gradients of the electron beam and wiggler field. These processes manifest themselves as changes in the harmonic power and transverse intensity profile. A transverse source function for the monochromatic radiation from a single electron in a plane-polarized wiggler magnetic field is derived that addresses these various effects. The resultant source is a composite of multiply peaked sources distributed over the local transverse wiggle range of each electron where the nth source has n peaks. For transverse-electron-beam density distributions that are slowly varying, an excellent description of the harmonic radiation can be obtained by including only the first few sources. Transverse averages of the distributed sources are taken to make comparisons with previous one-dimensional theories where they exist.

I. INTRODUCTION

In contrast with conventional lasers, the radiation from free-electron lasers (FEL's) is generated by individual electrons as they execute macroscopic transverse oscillations in a periodic magnetic field. The spatial amplitude of these oscillations can be much greater than the FEL radiation wavelength. Consequently, the electron radiation source can have structure over its oscillating range. The structure appears as variations in the electrons' radiation phase at different transverse positions along its trajectory. Thus, each electron can be thought of as a *distributed* radiation source with a radiation source pattern that is different for each harmonic. In this paper we obtain an expression for the distributed monochromatic radiation source pattern of an electron in a plane-polarized wiggler magnetic field.

Previous one-dimensional (1D) classical[1-3] and quantum-mechanical[4,5] analyses of the source functions for the fundamental and harmonic radiation in FEL's obtain a result that is equivalent to the transverse average of the distributed source function discussed herein. The 1D coupling coefficients ignore the multiply peaked nature of the harmonic source functions by discarding the oscillating terms in their mathematical expansion. Disposing of these terms would be justified if the electron radiated at a single transverse position in space. However, since the electron oscillates in transverse space with oscillation frequency equal to an integer divisor of the frequency of the oscillating terms, coherent enhancement over many wiggler periods will occur. Therefore these oscillating terms must be considered so that their contribution to the total harmonic radiation can be ascertained.

The single-electron source pattern is of fundamental importance in determining the radiation pattern of an ensemble of electrons in a FEL. The radiation pattern of an electron beam is determined by the convolution of the single-electron source pattern with the transverse density of the electron beam. The description embraces two notable limiting cases. For filamentary electron beams the resultant radiation source will be a scaled version of the single-electron source. Alternatively, in the limit of an infinitely wide electron beam, the radiation source will be given by a scaled version of the transverse average of the distributed single-electron source, i.e., the one-dimensional description.

In Sec. II the form of the distributed transverse source function of a single electron for arbitrary harmonic number is derived including misalignment effects. A higher-γ approximation is invoked to simplify the analysis. In Sec. III the 1D FEL coupling coefficients are recovered by performing a transverse average of the source functions derived in Sec. II. Such an average eliminates coupling to the even harmonics for an aligned system. In Sec. IV a discrete form of the distributed source function is constructed to allow the multiply peaked nature of the harmonic radiation to be modeled numerically. This analysis also gives insight into the relative amplitudes of the even and odd harmonic radiation. Modifications of the formalism to include the effects of transverse drift velocities and transverse gradients in the wiggler magnetic field are also discussed. The conclusions are given in Sec. V.

II. COLLAPSED SOURCE FUNCTIONS

The paraxial wave equation can be expressed[6-8]

$$\left[2ifk_s\frac{d}{dz}+\frac{\partial^2}{\partial\bar{r}_\perp^{\,2}}\right]E_\perp^f=S(x,y,z)\ , \tag{1}$$

where f is the harmonic number, $E_\perp^f$ is the transverse electric field phasor of the fth harmonic, and $k_s=2\pi/\lambda_s$ is the wave number of the fundamental. Bunching of the electron beam gives rise to coherent radiation that is driven by the source term $S(x,y,z)$ given in cgs units by

$$S(x,y,z)=-\frac{i8\pi f k_s}{\lambda_s c}\int_z^{z+\lambda_s} d\zeta\, J_\perp(x,y,\zeta)e^{-if(k_s\zeta-\omega_s t)}\ , \tag{2}$$

where $J_\perp$ is the transverse current defined by the discrete electron distribution. The integral in this equation can be interpreted as the projection, out of the total transverse current, of the transverse driving current at the optical wavelength.

A rigorous expression for the transverse current includes the transverse drift velocities of the individual electrons. Such an expression has the form

$$\mathbf{J}_\perp(x,y,z)=-e\sum_{i=1}^{N}\mathbf{v}_{\perp i}\delta(z-z_i(t))\delta(x-x_{0i}-\beta_{x0i}z)\times\delta(y-y_{0i}-\beta_{y0i}z-\chi_i\sin(k_w z))\ , \tag{3}$$

where (x_{0i},y_{0i}) and $(\beta_{x0i},\beta_{y0i})$ are the transverse guiding center position and normalized drift velocities of the ith electron, respectively. Here e is the magnitude of the charge of an electron such that its sign is expressed explicitly. The summation limit N represents the number of electrons in an optical (more precisely, ponderomotive) wavelength. The transverse velocity $\mathbf{v}_{\perp i}$ is given by[3]

$$\mathbf{v}_{\perp i}=\hat{\mathbf{x}}\beta_{x0i}c+\hat{\mathbf{y}}\left[\frac{a_{wi}}{\gamma_i}+\beta_{y0i}\right]c\ , \tag{4}$$

where $a_{wi}=[a_w(x,y,z)]_i$ is the wiggler magnetic vector potential at the guiding center of the ith electron which incorporates both axial and transverse field dependences. As seen from the third δ function in Eq. (3), it has been assumed that the wiggler magnetic field is the x direction with the dependence $\mathbf{B}=\hat{\mathbf{x}}B_w\sin(k_w z)$ such that the electrons wiggle in the y direction. Assuming $\gamma\gg a_w$, the betatron wavelength[9] will be much greater than the wiggler wavelength, and betatron motion can be linearized over a wiggler wavelength. An electron's transverse position is then given by

$$\begin{aligned} y&=y_{0i}+\chi_i\sin(k_w z)+\beta_{y0i}z\ ,\\ x&=x_{0i}+\beta_{x0i}z\ , \end{aligned} \tag{5}$$

where

$$\chi_i=\frac{a_w(x_{0i},y_{0i})}{\gamma_i k_w} \tag{6}$$

is equal to the oscillation amplitude of the ith electron to $O(1/\gamma^2)$. The linearized betatron drifts in Eq. (5) oscillate as the electron executes a betatron oscillation. When considering well-matched electron beams with smoothly varying transverse symmetry, the contribution to the radiated power from that portion of the transverse current ($J_\perp$) caused by the transverse drift velocities[10] is insignificant, as shown in Appendix A. However, the transverse drift velocities modify the axial electron velocity and the electron's phase in the optical wave. These modifications are incorporated in Eq. (9) below and are defined in the expressions of Appendix B.

With the caveats of Appendix A in mind, the transverse current can be approximated by

$$J_\perp(x,y,z)\simeq -ec\sum_{i=1}^{N}\frac{a_{wi}}{\gamma_i}\delta(z-z_i(t))\delta(x-x_{0i})\times\delta(y-y_{0i}-\chi_i\sin(k_w z))\ . \tag{7}$$

Substituting Eq. (7) into Eq. (2), the integration over ζ can be performed. Examining this expression for the ith electron we have

$$S_i(x,y,z_i)=\frac{i8\pi e f k_s}{\lambda_s}\delta(x-x_{0i})\times\delta(y-y_{0i}-\chi_i\sin(k_w z_i))\times\frac{a_w(x,y)}{\gamma_i}\cos k_w z_i e^{-if(k_s z_i-\omega_s t)}\ . \tag{8}$$

As discussed in Appendix B, the expression for the electron's axial position can be split into two terms $z_i(t)=\bar{z}_i(t)-\Delta z(t)$, where $\bar{z}_i(t)$ is the axial location assuming the electron has uniform axial velocity (as it would in a helical wiggler) and $\Delta z(t)$ is the oscillating correction term arising from the plane-polarized wiggler magnetic field, given by

$$\Delta z(t)=\frac{\xi}{k_s}\sin[2k_w\bar{z}_i(t)]+\frac{\sigma}{k_s}\sin[k_w\bar{z}_i(t)]\ , \tag{9}$$

where ξ is the interaction strength parameter[3] defined in Eq. (B14), and σ is the angular coupling parameter defined in Eq. (B15). The Z parameter defined by Colson, Dattoli, and Ciocci[3] is equal to our parameter σ if one assumes $\beta_z\simeq 1$ and only small-angle misalignments ($\sin\theta\simeq\theta$) in the wiggle plane are being considered. Nonzero σ is caused by misalignment of an individual electron's guiding center trajectory with the wiggler axis. Such a misalignment can arise as a result of gross electron-beam misalignment into the wiggler, focusing of the electron beam, wiggler field errors, and betatron motion.

One can see from Eqs. (8) and (9) that the single-electron source function is periodic in z_i, with period λ_w. By averaging over this length we can obtain a "collapsed" multipole single-electron source function that is distributed over the electron's wiggle amplitude in the y direction. Using Eqs. (B8) and (9) in (8), the y-dependent source function becomes

$$S_i(y)=\frac{i8\pi e f k_s}{\lambda_s\lambda_w}\delta(x-x_{0i})\oint d\bar{z}_i\,\delta(y-y_{0i}-\chi_i\sin[k_w(\bar{z}_i+\Delta z)])\times\cos[k_w(\bar{z}_i+\Delta z)]\frac{a_w(x,y)}{\gamma_i}\exp\{-if[k_s\bar{z}_i-\xi\sin(2k_w\bar{z}_i)-\sigma\sin(k_w\bar{z}_i)-\omega_s t]\}\ , \tag{10}$$

where $\oint d\bar{z}_i(t)$ indicates an integral of $\bar{z}_i(t)$ over a complete wiggler wavelength. As shown in Appendix B, the $k_w\Delta z$ correction term in the cosine and δ-function arguments can be ignored so that

$$S_i(y)=\frac{i8\pi efk_s}{\lambda_w\lambda_s}a_w(x_{0i},y)\delta(x-x_{0i})\oint d\bar{z}_i\delta(y-y_{0i}-\chi_i\sin(k_w\bar{z}_i))\frac{\cos(k_w\bar{z}_i)}{\gamma_t}\exp\{-if[(k_s+k_w)\bar{z}_i-\omega_s t]\}$$
$$\times\exp\{if[\xi\sin(2k_w\bar{z}_i)+\sigma\sin(k_w\bar{z}_i)+k_w\bar{z}_i]\}\ , \tag{11}$$

where we have subtracted and added $ifk_w\bar{z}_i$ in the two exponential terms, respectively. The first exponential term can be recognized as the resonant phase of the ith electron or

$$\psi_i=(k_s+k_w)\bar{z}_i(t)-\omega_s t\ , \tag{12}$$

which is constant at resonance. Assuming γ_i does not change significantly over a wiggler wavelength, we can pull it and the resonant exponential outside the integral giving

$$S_i(y)=\frac{i8\pi efk_s}{\lambda_w\lambda_s}a_w(x_{0i},y)\frac{e^{-if\psi_t}}{\gamma_i}\delta(x-x_{0i})$$
$$\times\oint d\bar{z}_i\delta(y-y_{0i}-\chi_t\sin(k_w\bar{z}_i))\cos(k_w\bar{z}_i)\exp\{if[\xi\sin(2k_w\bar{z}_i)+\sigma\sin(k_w\bar{z}_i)+k_w\bar{z}_i]\}\ . \tag{13}$$

To evaluate the $\bar{z}_i(t)$ integral we use the relation

$$\delta(f(z))=\sum_r\frac{\delta(z-z_r)}{\left|\frac{df}{dz}(z_r)\right|}\ , \tag{14}$$

where the sum indicates a summation of all the roots of $f(z)=y-y_{0i}-\chi_i\sin(k_w\bar{z}_i)$, so that

$$S_i(y)=\frac{i8\pi efk_s}{\lambda_w\lambda_s}a_w(x_{0i},y)\frac{e^{-if\psi_t}}{\gamma_i}\delta(x-x_{0i})\oint d\bar{z}_i\sum_r\frac{\delta(\bar{z}_i-z_{ri})}{k_w\chi_i}\frac{\cos(k_w\bar{z}_i)}{|\cos(k_w\bar{z}_i)|}\exp\{if[\xi\sin(2k_w\bar{z}_i)+\sigma\sin(k_w\bar{z}_i)+k_w\bar{z}_i]\}\ . \tag{15}$$

At this point we split the integral into two subintegrals to eliminate the ratio of cosines and account for the two z roots at each transverse y location. Since the cosine ratio is negative between $\lambda_w/4$ and $3\lambda_w/4$, we have

$$S_i(y)=\frac{i4efk_s}{\lambda_s}a_w(x_{0i},y)\frac{e^{-if\psi_t}}{\chi_i\gamma_t}$$
$$\times\left[-\int_{\lambda_w/4}^{3\lambda_w/4}d\bar{z}_i\delta(\bar{z}_i-z_{2i})\exp\{if[\xi\sin(2k_w\bar{z}_i)+\sigma\sin(k_w\bar{z}_i)+k_w\bar{z}_i]\}\right.$$
$$\left.+\int_{-\lambda_w/4}^{\lambda_w/4}d\bar{z}_i\delta(\bar{z}_i-z_{1i})\exp\{if[\xi\sin(2k_w\bar{z}_i)+\sigma\sin(k_w\bar{z}_i)+k_w\bar{z}_i]\}\right]\delta(x-x_{0i})\ . \tag{16}$$

From Eq. (5a) we see that the roots are given by

$$z_{1i}=\frac{1}{k_w}\sin^{-1}\left[\frac{y-y_{0i}}{\chi_t}\right] \tag{17}$$

in the region $-\lambda_w/4$ to $\lambda_w/4$ and by

$$z_{2i}=\frac{1}{k_w}\left[\pi-\sin^{-1}\left[\frac{y-y_{0i}}{\chi_i}\right]\right] \tag{18}$$

in the region $\lambda_w/4$ to $3\lambda_w/4$. The transverse source function can now be written as

$$S_i(y)=\frac{i4efk_s}{\lambda_s}a_w(x_{0i},y)\frac{e^{-if\psi_i}}{\chi_i\gamma_i}(-\exp\{if[\xi\sin(2k_wz_{2i})+\sigma\sin(k_wz_{2i})+k_wz_{2i}]\}$$
$$+\exp\{if[\xi\sin(2k_wz_{1i})+\sigma\sin(k_wz_{1i})+k_wz_{1i}]\})\delta(x-x_{0i})\ , \tag{19}$$

or defining

$$\theta_r=\sin^{-1}\left[\frac{y-y_{0i}}{\chi_i}\right] \tag{20}$$

we have

$$S_i(y)=\frac{i4efk_s}{\lambda_s}a_w(x_{0i},y)\frac{e^{-if\psi_i}}{\chi_i\gamma_i}\delta(x-x_{0i})\exp\{if[\xi\sin(2\theta_i)+\sigma\sin\theta_i+\theta_i]\}\Big|_{\theta_i=\pi-\theta_r}^{\theta_i=\theta_r}. \tag{21}$$

Now, since $\sin[2(\pi-\theta_r)]=-\sin(2\theta_r)$, the previous equation becomes

$$S_i(y)=\frac{i4efk_s}{\lambda_s}a_w(x_{0i},y)\frac{e^{-if\psi_i}}{\chi_i\gamma_i}\delta(x-x_{0i})(\exp\{if[\xi\sin(2\theta_r)+\theta_r]\}-\exp\{-if[\xi\sin(2\theta_r)-\pi+\theta_r]\})e^{if\sigma\sin\theta_r}. \tag{22}$$

Using Eq. (6) and noting the implicit dependence of θ_r on y through Eq. (20), the single-electron source at the odd harmonics becomes

$$S_i^o(y)=\frac{i8efk_sk_w}{\lambda_s}e^{-if\psi_i}\delta(x-x_{0i})\times\cos\{f[\xi\sin(2\theta_r)+\theta_r]\}e^{if\sigma\sin\theta_r}, \tag{23}$$

and for the even harmonics

$$S_i^e(y)=-\frac{8efk_sk_w}{\lambda_s}e^{-if\psi_i}\delta(x-x_{0i})\times\sin\{[\xi\sin(2\theta_r)+\theta_r]\}e^{if\sigma\sin\theta_r}. \tag{24}$$

As seen from Eq. (20), these equations are only valid for

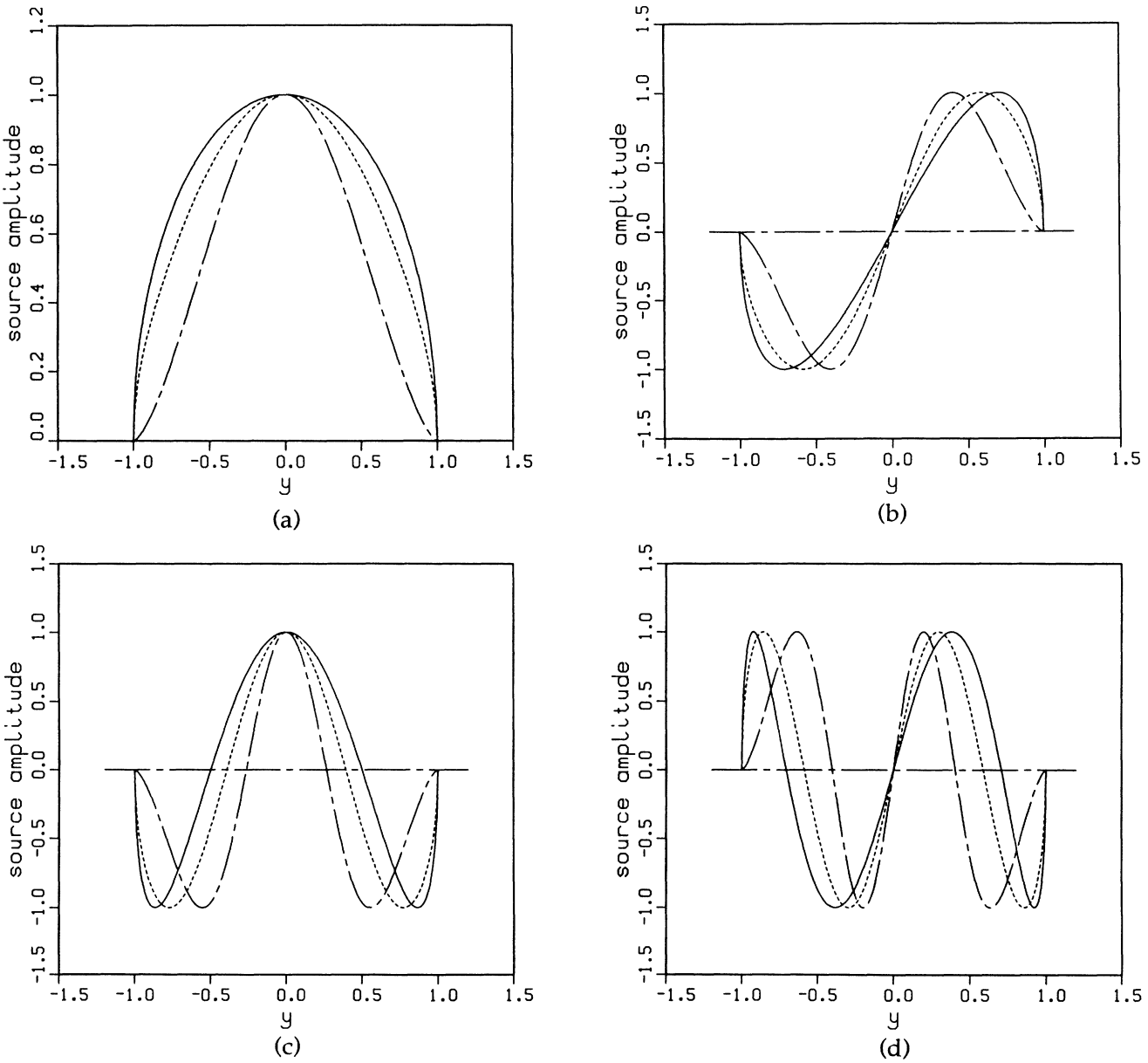

FIG. 1. (a)–(d) Plots of the normalized transverse source dependence in the limit $\sigma=0$ for the fundamental and first three harmonics. The three curves in each plot represent the source for $\xi=10^{-5}$ (solid curve), $\xi=\frac{1}{6}$ (dotted curve), and $\xi=\frac{1}{2}$ (dot-dashed curve). These values of ξ correspond to a_w values of 0.01, 1, and ∞, respectively.

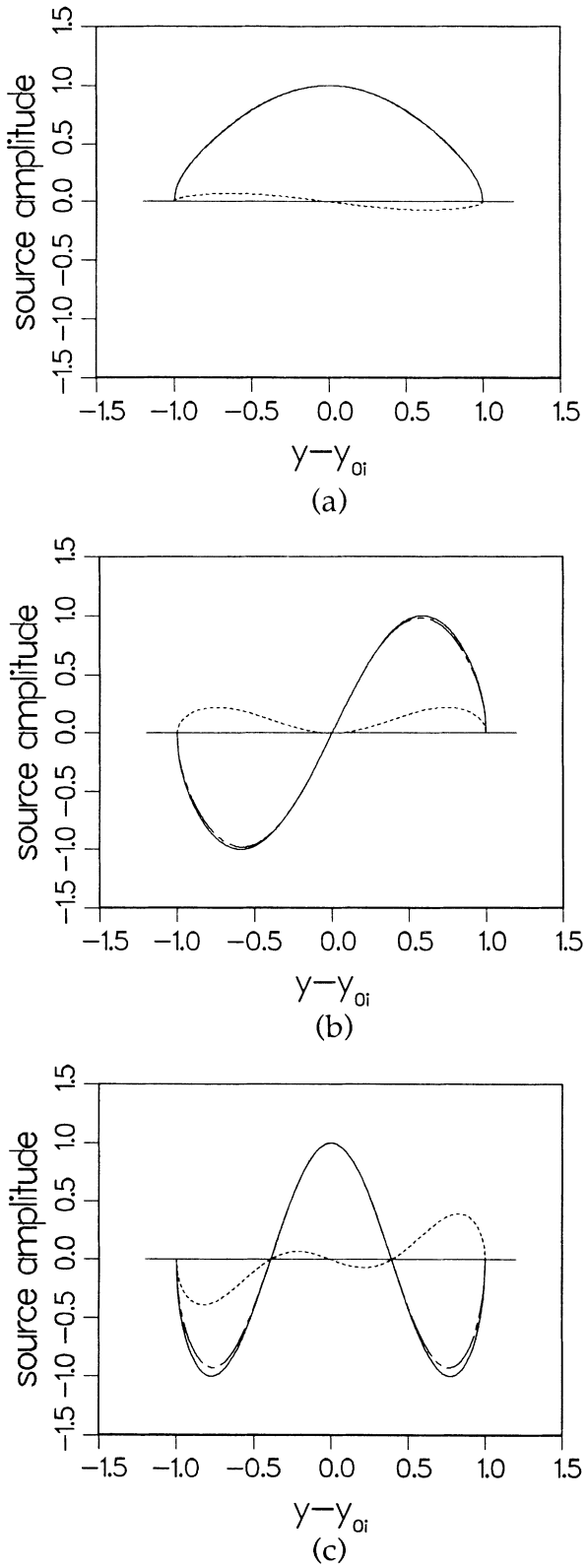

FIG. 2. (a)–(c) Plots of the source functions including angular effects with $\sigma=\xi=\frac{1}{6}$ for the fundamental, second, and third harmonic. The real and imaginary parts have been plotted with dot-dashed and dotted lines, respectively. For reference, the solid line plots the source function for $\sigma=0$. Note that the large imaginary part introduces a source with opposite symmetry from the $\sigma=0$ reference case.

$y_{0i}-\chi_i \le y \le y_{0i}+\chi_i$ (since this is the spatial range of the ith electron). It was assumed in going from Eq. (22) to Eqs. (23) and (24) that $a_w(x_{0i},y_{0i})=a_w(x_{0i},y)$. This is a good assumption since the electron wiggle amplitude is much smaller than the transverse wiggler field gradient length. The gradient of the transverse wiggler field also produces coupling to the even harmonics. The extent of this coupling is explored in Appendix C and is shown to be small for conventional FEL's. These equations express the explicit radiation source amplitudes as a function of transverse position for a single electron. It is interesting to note that in the limit $\sigma \to 0$ the resonant source functions [the term in bold parentheses in Eq. (22)] go from complex to purely real or purely imaginary quantities. Insight into this characteristic can be gained by noting from Eq. (22) that the source function is complex at each transverse y location (even for $\sigma=0$). However, the electrons traverse each y location twice (but at different z locations) per wiggler wavelength, and it is the sum of the source functions for these two different axial locations that forms the resultant source function at each transverse location. In the limit $\sigma=0$, the electron has the opposite transverse velocity at the second location relative to the first, such that the source functions at the two locations are complex conjugates. As a result, their sum is no longer complex at any transverse position.

Note that Eqs. (23) and (24) have no exhibited dependence on the wiggler magnetic vector potential. This dependence is hidden in ξ, σ, and θ_r as one can see from Eqs. (B14), (B15), (20), and (6).

The source functions can be plotted to obtain the exact transverse radiation pattern for each harmonic for a specific interaction strength ξ. Figures 1(a)–1(d) give the normalized transverse source dependence in the limit $\sigma=0$ for the fundamental and first three harmonics. The three curves in each plot represent the source for $\xi=10^{-5}$ (solid curve), $\xi=\frac{1}{6}$ (dotted curve), and $\xi=\frac{1}{2}$ (dot-dashed curve). These values of ξ correspond to a_w values of 0.01, 1, and ∞, respectively. Plots of the source functions including angular effects with $\sigma=\xi=\frac{1}{6}$ are given in Figs. 2(a)–2(c) for the fundamental, second, and third harmonic. Since the source functions are now complex, we have plotted their real and imaginary parts with dot-dashed and dotted lines, respectively. For reference, the solid line plots the source function for $\sigma=0$. Note that the real part of the source function is only slightly modified from its $\sigma=0$ value despite the large value of σ assumed for these calculations.

III. RELATION OT THE COUPLING COEFFICIENTS

To link this theory with the simplified coupling coefficients derived by others[3] we take the integral of the transverse source function for an individual electron over its range. The integral over x is trivial due to the δ-function dependence, leaving

$$\bar{S}_i = \int_{y_{0i}-\chi_i}^{y_{0i}+\chi_i} dy\, S_i(y) \ , \tag{25}$$

where we do not normalize the integral since we are interested in the net source, i.e., the area under the curve.

Now, since we are assuming $y-y_{0i}\simeq\chi_i\sin\theta_r$ [see Eq. (5)], we can make a change of variable to θ_r where $dy=\chi_i\cos\theta_r d\theta_r$. The integral limits become

$$\theta_1=\sin^{-1}(-1)=-\pi/2\ ,\qquad \theta_2=\sin^{-1}(1)=\pi/2\ , \tag{26}$$

where the 1 and 2 subscripts represent the beginning and end of the integration, respectively. Now, substituting in from Eqs. (23) and (24) gives

$$\left.\begin{matrix}\bar{S}_i^o\\ \bar{S}_i^e\end{matrix}\right\}=\frac{i8efk_sk_w}{\lambda_s}e^{-if\psi_i}\chi_i\int_{-\pi/2}^{\pi/2}\cos\theta_r d\theta_r\times\begin{Bmatrix}\cos\\ -\sin\end{Bmatrix}\{f[\xi\sin(2\theta_r)+\theta_r]\}\times\begin{Bmatrix}\cos\\ \sin\end{Bmatrix}(f\sigma\sin\theta_r)$$

$$=\frac{i8efk_sk_w\chi_i}{\lambda_s}e^{-if\psi_i}\times\begin{Bmatrix}\mathrm{Re}\\ \mathrm{Im}\end{Bmatrix}\int d\theta_r\left[\frac{e^{i\theta_r}+e^{-i\theta_r}}{2}\right]e^{if[\xi\sin(2\theta_r)+\theta_r]}\times\begin{Bmatrix}\cos\\ -\sin\end{Bmatrix}(f\sigma\sin\theta_r)$$

$$=\frac{i4efk_sk_w\chi_i}{\lambda_s}e^{-if\psi_i}\times\begin{Bmatrix}\mathrm{Re}\\ \mathrm{Im}\end{Bmatrix}\int d\theta_r(e^{i(f+1)\theta_r}+e^{i(f-1)\theta_r})e^{if\xi\sin(2\theta_r)}\times\begin{Bmatrix}\cos\\ -\sin\end{Bmatrix}(f\sigma\sin\theta_r)\ . \tag{28}$$

Using the expansion

$$e^{if\xi\sin(2\theta_r)}=\sum_{n=-\infty}^{\infty}J_n(f\xi)e^{i2n\theta_r}\ , \tag{29}$$

Eq. (28) becomes

$$\left.\begin{matrix}\bar{S}_i^o\\ S_i^e\end{matrix}\right\}=\frac{i4efk_sk_w\chi_i}{\lambda_s}e^{-if\psi_i}\times\begin{Bmatrix}\mathrm{Re}\\ \mathrm{Im}\end{Bmatrix}\sum_{n=-\infty}^{\infty}J_n(f\xi)\int_{-\pi/2}^{\pi/2}d\theta_r(e^{i(f+2n+1)\theta_r}+e^{i(f+2n-1)\theta_r})\times\begin{Bmatrix}\cos\\ -\sin\end{Bmatrix}(f\sigma\sin\theta_r)\ . \tag{30}$$

Again invoking symmetry we have

$$\left.\begin{matrix}\bar{S}_i^o\\ \bar{S}_i^e\end{matrix}\right\}=\frac{i4efk_sk_w\chi_i}{\lambda_s}e^{-if\psi_i}\sum_{n=-\infty}^{\infty}J_n(f\xi)\left[\int_{-\pi/2}^{\pi/2}d\theta_r\times\begin{Bmatrix}\cos\\ \sin\end{Bmatrix}[(f+2n+1)\theta_r]\times\begin{Bmatrix}\cos\\ -\sin\end{Bmatrix}(f\sigma\sin\theta_r)\right.$$

$$\left.+\int_{-\pi/2}^{\pi/2}d\theta_r\times\begin{Bmatrix}\cos\\ \sin\end{Bmatrix}[(f+2n-1)\theta_r]\times\begin{Bmatrix}\cos\\ -\sin\end{Bmatrix}(f\sigma\sin\theta_r)\right]\ , \tag{31}$$

and evaluating the integrals[11] gives

$$\bar{S}_i=\frac{i4\pi efk_sk_w\chi_i}{\lambda_s}e^{-if\psi_i}(-1)^{f+1}\times\sum_{n=-\infty}^{\infty}J_n(f\xi)[J_{2n+f+1}(f\sigma)+J_{2n+f-1}(f\sigma)]\ , \tag{32}$$

which is valid for both even and odd harmonics. Making the following definitions:

$$\langle\cdots\rangle_e=\frac{1}{N}\sum_{i=1}^{N}(\cdots)\ , \tag{33}$$

$$\mathcal{K}_f^{(m)}(\xi,\sigma)=(-1)^f\sum_{n=-\infty}^{\infty}J_n(f\xi)[(-1)^mJ_{2n+f-m}(f\sigma)-J_{2n+f+m}(f\sigma)]\ , \tag{34}$$

$$\left.\begin{matrix}\bar{S}_i^o\\ \bar{S}_i^e\end{matrix}\right\}=\frac{i8efk_sk_w}{\lambda_s}e^{-if\psi_i}\times\int_{-\pi/2}^{\pi/2}\chi_i\cos\theta_r d\theta_r\times\begin{Bmatrix}\cos\\ i\sin\end{Bmatrix}\{f[\xi\sin(2\theta_r)+\theta_r]\}\times e^{if\sigma\sin\theta_r}\ , \tag{27}$$

where the upper (lower) operator should be used to evaluate the odd- (even-) harmonic result. From symmetry considerations we have

$$I\simeq\frac{eN}{\lambda_s}c\ , \tag{35}$$

we obtain the final expression for an ensemble of electrons

$$\bar{S}=\left\langle\frac{i4\pi Ifk_sa_{wi}}{c}\mathcal{K}_f^{(1)}(\xi,\sigma)\frac{e^{-if\psi}}{\gamma}\right\rangle_e\ , \tag{36}$$

which agrees with previous 1D theories.[3] The coupling coefficient in Eq. (34) is in agreement with that in Ref. 3 for $m=1$ and $\sigma\rightarrow-\sigma$ (required due to the different phase convention between the wiggle and drift motions). It is interesting to note that coupling coefficients can also be expressed in terms of a sum of two generalized Bessel functions,[5,12] i.e.,

$$\mathcal{K}_f^{(m)}(\xi,\sigma)=C_{f+m}(f\sigma,f\xi,0)+C_{f-m}(f\sigma,f\xi,0)\ , \tag{34'}$$

where the expression for $C_M(a,b,\theta)$ is given elsewhere.[12]

The dependence of the source function on the angle an electron makes with the wiggler axis appears only in the coupling coefficients defined in Eq. (34). In the limit of zero transverse drift, $\sigma \rightarrow 0$ and Eqs. (34) and (34′) become

$$\mathcal{H}_f^{(1)}(\xi)=(-1)^{(f-1)/2}[J_{(f-1)/2}(f\xi)-J_{(f+1)/2}(f\xi)] , \tag{37}$$

which only has nonzero amplitude at the odd-harmonic frequencies. Thus, for aligned systems, the even-harmonic radiation has been averaged away. In the next section we described a process by which the even-harmonic interaction is retained.

IV. MULTIPOLE SOURCES

In Sec. III we showed that by averaging the collapsed transverse source function over y we obtained the 1D coupling coefficients. In this section, we want to retain the multipole nature of the single-electron radiation pattern in a form that is amenable to numerical simulation. To model the "collapsed" source terms in Eqs. (23) and (24) we can convert the smoothly varying analytical form into a discrete δ-function multipole source term that can be more efficiently modeled on a transverse grid. To exactly model the analytic source function requires an infinite sum of discrete multipole sources. We will show that under certain conditions (generally satisfied in practice) only the lowest-order multipoles need be kept. The resultant transverse source will then be determined by the discrete source function for each electron and the distribution of the electrons in transverse space, i.e., the transverse density $n(y)$. Since the electrons only wiggle in the y direction, we assume the transverse source in the x direction to be singular (δ-function source located at the electron positions in x) while the source is distributed in y due to the electron wiggle motion. Simulation of the harmonic radiation from a helically polarized FEL requires a distributed source in both x and y. Since the x analysis is identical (within a phase factor) to the derivation for a distributed source in y, we will not complicate the analysis by including it here.

To determine the y dependence of the resultant source, we impose two conditions in order to make a discrete multipole source equivalent to the analytic source. First, the electron density must be smoothly varying over the amplitude of the electron's wiggler motion. This condition is easily satisfied for high-γ FEL's where the electron-beam wiggle amplitude is much less than the radius of the electron beam. The second condition requires that the proper weights be given to each of the δ-function poles. The appropriate weights can be calculated by evaluating the resultant source obtained using the continuous source functions given in Eqs. (23) and (24) and equating them with the results obtained using discrete δ-function multipole sources.

We want to find the resultant source $\mathcal{S}(y)$ due to a transverse density $n(y_{0i})$ and a distributed single-electron source $S(\Delta y)$ as depicted in Fig. 1. If we imagine a singular transverse density of $n(y_{0i})=\delta(y_{0i}-y_2)$, then the resultant source at position y must be given by $\mathcal{S}(y-y_2)$. Therefore, for arbitrary $n(y_{0i})$, the resultant source must be given by

$$\mathcal{S}(y)=\int_{y-\chi_i}^{y+\chi_i} S(y-y_{0i})n(y_{0i})dy_{0i} , \tag{38}$$

where $n(y_{0i})$ is the normalized transverse density such that

$$\int_{-\infty}^{\infty} dy_{0i} n(y_{0i})=1 . \tag{39}$$

Assuming that $n(y_{0i})$ is slowly varying over an electron's wiggle amplitude χ_i, the density can be expanded in a Taylor series so that

$$\mathcal{S}(y)=\int_{y-\chi_i}^{y+\chi_i} S(y-y_{0i})[n(y)+(y_{0i}-y)n'(y) + \cdots]dy_{0i} . \tag{40}$$

The first term in this series has already been evaluated in another form in Eq. (32) of Sec. II, with the result

$$\mathcal{S}_1=-i\frac{\pi}{2}Cn(y)\chi_i\mathcal{H}_f^{(1)}(\xi,\sigma) , \tag{41}$$

where we have grouped the constant coefficients into the C term given by

$$C\equiv\frac{8iefk_s k_w}{\lambda_s}e^{-if\psi_i} , \tag{42}$$

and $\mathcal{H}_f^{(1)}(\xi,\sigma)$ has been defined in Eq. (34). The 1 subscript in Eq. (41) signifies that this is the source due to the first term in the expansion.

The discrete source for the odd harmonics is applied on the numerical grid at the guiding center position of each electron. This source is given by

$$S_1^{\dagger}=W_1\delta(y-y_{0i}) , \tag{43}$$

where the dagger superscript identifies the discrete nature of the source. This expression can be substituted into Eq. (38) and the integral performed to obtain the resultant source for the first term in the density expansion yielding

$$\mathcal{S}_1^{\dagger}=W_1 n(y) . \tag{44}$$

Solving for W_1 from Eqs. (41) and (44), and substituting back into Eq. (43) gives

$$\mathcal{S}_1^{\dagger}=i2efk_s^2 a_{w1}\frac{e^{-if\psi_i}}{\gamma_i}\mathcal{H}_f^{(1)}(\xi,\sigma)\delta(y-y_{0i}) . \tag{45}$$

Note that for perfect alignment ($\sigma \rightarrow 0$) the coupling coefficients exist only at the odd-harmonic frequencies. The source for the even harmonics contributed by the first term of the series vanished due to the odd symmetry of their distributed sources.

One must evaluate the second term of the density expansion to obtain the dominant source term for the even harmonics in the absence of misalignment. From Eqs. (23) and (24), the single-electron sources, including misalignment effects, are given by

$$S_i(y-y_{0i})=C\times\begin{Bmatrix}\cos\\ i\sin\end{Bmatrix}(f\{\xi\sin[2\theta_r(y-y_{0i})]+\theta_r(y-y_{0i})\})\times e^{if\sigma\sin\theta_r(y-y_{0i})}. \quad (46)$$

Using Eq. (46) in (40) gives

$$\mathcal{S}=C\int_{y-\chi_i}^{y+\chi_i}\begin{Bmatrix}\cos\\ i\sin\end{Bmatrix}\{f[\xi\sin2\theta_r(y-y_{0i})+\theta_r(y-y_{0i})]\}\times e^{if\sigma\sin[\theta_r(y-y_{0i})]}\times[n(y)+(y_{0i}-y)n'(y)+\cdots]dy_{0i}. \quad (47)$$

Concentrating on the second term in the expansion gives

$$\mathcal{S}_2=Cn'(y)\int_{\pi/2}^{-\pi/2}\begin{Bmatrix}\cos\\ i\sin\end{Bmatrix}[f(\xi\sin2\theta_r+\theta_r)]e^{if\sigma\sin\theta_r}\chi_i\sin\theta_r\chi_i\cos\theta_r d\theta_r$$
$$=-iCn'(y)\frac{\chi_i^2}{2}\int_{-\pi/2}^{\pi/2}\begin{Bmatrix}\cos\\ \sin\end{Bmatrix}[f(\xi\sin2\theta_r+\theta_r)]\times\begin{Bmatrix}\sin\\ \cos\end{Bmatrix}(f\sigma\sin\theta_r)\sin2\theta_r d\theta_r. \quad (48)$$

The integral in Eq. (48) is very similar to that in Eq. (27) and can be evaluated in an analogous fashion yielding

$$\mathcal{S}_2=-iC\pi n'(y)\frac{\chi_i^2}{4}\mathcal{H}_f^{(2)}(\xi,\sigma), \quad (49)$$

where $\mathcal{H}_f^{(2)}(\xi,\sigma)$ is defined in Eq. (34). In the limit $\sigma\to0$, the coupling term becomes

$$\mathcal{H}_f^{(2)}(\xi,\sigma\to0)=(-1)^{(f-2)/2}[J_{(f-2)/2}(f\xi)-J_{(f+2)/2}(f\xi)], \quad (50)$$

which only gives coupling at the even harmonics.

For the discrete δ-function dipole source, the resultant source is given by

$$\mathcal{S}^\dagger(y)=\int_{y-\chi_i}^{y+\chi_i}S^\dagger(y-y_{0i})n(y_{0i})dy_{0i}. \quad (51)$$

With Fig. 3(a) in mind, we choose the discrete source for the second harmonic to be two δ functions of equal magnitude and opposite sign separated by a distance $2y_1$, where y_1 has yet to be defined. This is depicted in Fig. 3(b). We assume the transverse electron density is slowly varying over a electron's wiggle amplitude as shown in Fig. 4. Mathematically we have

$$S_2^\dagger(y-y_{0i})=W_2[\delta(y-y_{0i}-y_1)-\delta(y-y_{0i}+y_1)]. \quad (52)$$

Now, using Eq. (52) to evaluate the second term of Eq.

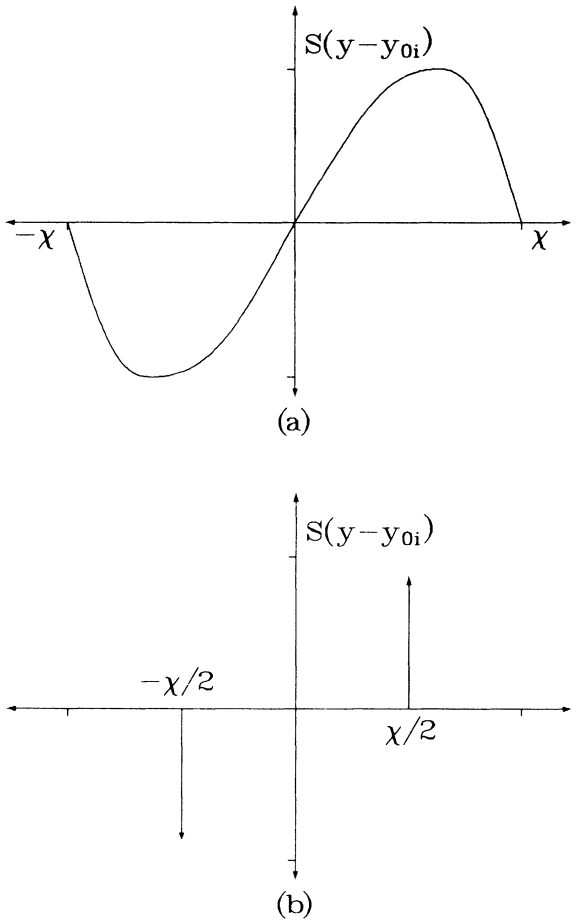

FIG. 3. (a)–(b) Analytic and discrete dipole source functions, respectively. The δ-function sources have been positioned half the distance from the guiding center to the wiggle extrema.

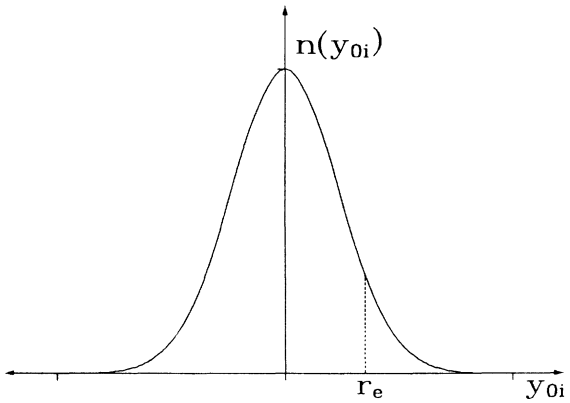

FIG. 4. Typical transverse electron-beam distribution. The electron-beam radius r_e is assumed to be much larger than the electron-beam wiggle amplitude χ.

(51) gives

$$\mathcal{S}_2^{\dagger}(y)=\int_{y-\chi_i}^{y+\chi_i} W_2[\delta(y-y_{0i}-y_1) -\delta(y-y_{0i}+y_1)]n(y_{0i})dy_{0i}$$

$$=W_2[n(y-y_1)-n(y+y_1)] . \quad (53)$$

Again expanding $n(y)$ in a Taylor series gives

$$\mathcal{S}_2^{\dagger}(y)=W_2\{[n(y)-y_1n'(y)+\cdots] -[n(y)+y_1n'(y)+\cdots]\}$$

$$=-2W_2y_1n'(y) . \quad (54)$$

To obtain the same resultant source for the discrete source as was obtained with the exact analytic source we equate Eqs. (49) and (54) yielding

$$2W_2y_1=i\frac{\pi}{4}C\chi_i^2\mathcal{H}_f^{(2)}(\xi,\sigma) , \quad (55)$$

and choosing

$$y_1=\chi_i/2 \quad (56)$$

gives

$$W_2=i\frac{\pi}{4}C\chi_i\mathcal{H}_f^{(2)}(\xi,\sigma) . \quad (57)$$

Therefore, using Eqs. (1), (33), (35), (42), (52), (56), and (57), the even-harmonic wave equation for an ensemble of electrons modeled as discrete dipole sources becomes

$$\left[2ifk_s\frac{d}{dz}+\frac{\partial^2}{\partial\bar{r}_\perp^2}\right]E_\perp^f$$

$$=-\left\langle\frac{4\pi Ifk_sa_{wi}}{c}\mathcal{H}_f^{(2)}(\xi,\sigma) \times\tfrac{1}{2}[\delta(y-y_{0i}-\chi/2)-\delta(y-y_{0i}+\chi/2)] \times\frac{e^{-if\psi}}{\gamma}\right\rangle_e . \quad (58)$$

Evaluation of the third term in the expansion which gives rise to tripole radiation is conducted in Appendix D. Note from Eqs. (54) and (D10) that the higher-order multipoles depend on higher derivatives of the transverse electron density profile. Thus, for smoothly varying transverse density profiles, sufficient accuracy can be obtained by including only the lowest two or three multipoles.

In order to model the coherent spontaneous emission of various FEL experiments, the distributed source model was implemented in the 3D code FELEX.[13] The most striking aspect of the simulation results is the odd symmetry of the transverse profile of the even harmonics. An example of this profile is given in Fig. 5 for the second harmonic of the Stanford Mark III oscillator. Bamford and Deacon[14] have measured the power radiated at the first six harmonics of the Stanford FEL. Good agreement between their measurements and the distributed source model results was achieved as reported in their paper. A more detailed description of harmonic simulations using the distributed source model and how they compare with experiment has been published elsewhere.[15]

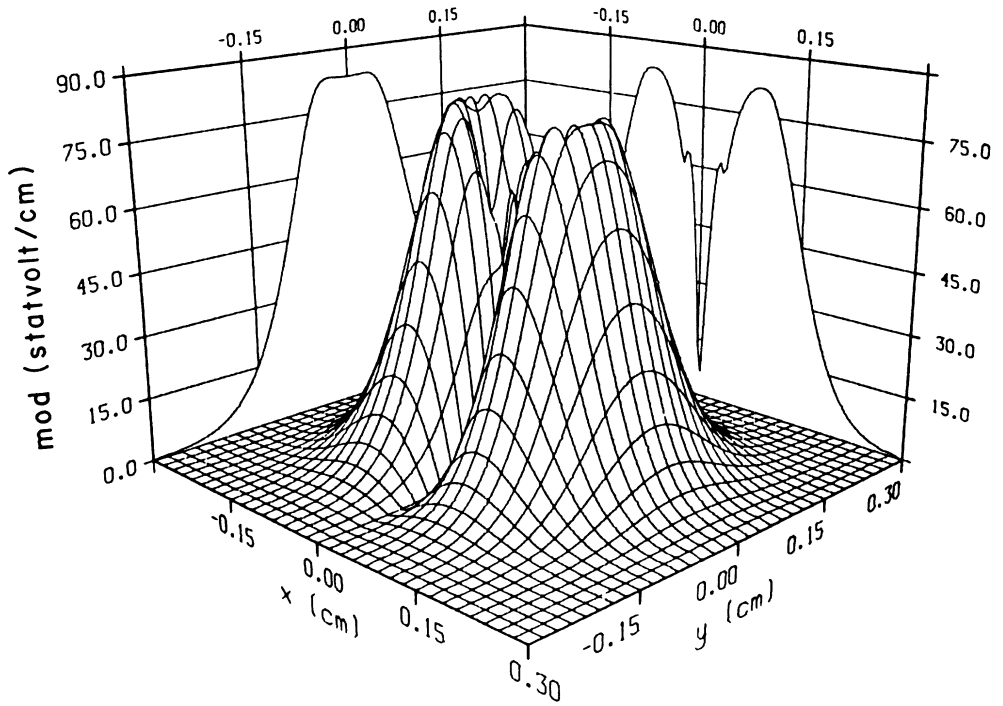

FIG. 5. Transverse electric field magnitude of the second harmonic at the wiggler exit for the Stanford Mark III oscillator. The negative amplitude of one of the lobes has been inverted for plotting purposes.

V. CONCLUSIONS

We have derived a formalism that more accurately describes the radiation in a free-electron laser at the fundamental and harmonic frequencies. Modifications to the harmonic radiation caused by transverse gradients in the wiggler magnetic field and misalignments of the electron guiding center trajectory with the wiggler axis have been included in the theory. The model assumes the electron radiates at only discrete frequencies. The radiation source is distributed over the transverse wiggle amplitude of each electron. When the distributed source function is averaged over transverse space, the simplified 1D results are recovered.

A discrete (δ-function) source function has been proposed for numerical modeling purposes. The discrete model requires the transverse-electron-beam density to be smoothly varying. The paraxial wave equation for the discrete model can be written

$$\left[2ifk_s\frac{d}{dz}+\frac{\partial^2}{\partial\bar{r}_\perp^{\,2}}\right]E_\perp^f = \sum_j^{1,2,3}\left\langle\frac{4\pi Ifk_s a_{wi}}{c}\mathcal{S}_j(y)\frac{e^{-if\psi}}{\gamma}\right\rangle_e , \quad (59)$$

where the three multipole source terms on the right-hand side are given by (i) the monopole term

$$\mathcal{S}_1(y)=i\mathcal{H}_f^{(1)}(\xi,\sigma)\delta(y-y_{0i}) , \quad (60)$$

(ii) the dipole term

$$\mathcal{S}_2(y)=-\mathcal{H}_f^{(2)}(\xi,\sigma)\tfrac{1}{2}[\delta(y-y_{0i}-\chi/2)-\delta(y-y_{0i}+\chi/2)] , \quad (61)$$

and (iii) the tripole term

$$\mathcal{S}_3(y)=-i[\mathcal{H}_f^{(1)}(\xi,\sigma)-\mathcal{H}_f^{(3)}(\xi,\sigma)]\times\{\delta(y-y_{0i})-\tfrac{1}{2}[\delta(y-y_{0i}-\chi/2)+\delta(y-y_{0i}+\chi/2)]\} , \quad (62)$$

and the expression for the coupling coefficients is given in Eq. (34). Additional monopole source contributions due to magnetic field gradients and mismatching of the electron beam have also been derived in Eq. (A8) and (C5), respectively. The distributed source model predicts the generation of even-harmonic radiation with odd symmetry in the electron wiggle plane (for perfectly aligned systems) and odd-harmonic radiation patterns with even transverse symmetry. Simulations of harmonic emission for present FEL devices show good agreement with experimental measurements.

ACKNOWLEDGMENTS

This work was performed under the auspices of the U.S. Department of Energy and partially supported by the U.S. Army Ballistic Missile Defense Organization.

APPENDIX A

We evaluate the radiation contribution from the transverse drift terms $(\beta_{x0i},\beta_{y0i})$, and show that often their contribution may be neglected. Substituting Eq. (3) into Eq. (2) gives

$$\mathbf{S}_i(x,y,z_i)=\frac{i8\pi efk_s}{\lambda_s}\delta(x-x_{0i}-\beta_{x0i}z)\times\delta(y-y_{0i}-\beta_{y0i}z-\chi_i\sin(k_w z_i))\times\left[\hat{\mathbf{x}}\beta_{x0i}+\hat{\mathbf{y}}\left[\frac{a_{wi}}{\gamma_i}\cos(k_w z_i)+\beta_{y0i}\right]\right]\times e^{-if(k_s z_i-\omega_s t)} , \quad (A1)$$

where the source has now become a vector quantity such that electric field amplitudes in both transverse directions will be generated. Specializing to sources caused solely by transverse drifts we have

$$\mathbf{S}_{\perp 0i}(x,y,z_i)=\frac{i8\pi efk_s}{\lambda_s}\delta(x-x_{0i}-\beta_{x0i}z)\times\delta(y-y_{0i}-\beta_{y0i}z-\chi_i\sin(k_w z_i))\times[\hat{\mathbf{x}}\beta_{x0i}+\hat{\mathbf{y}}\beta_{y0i}]e^{-if(k_s z_i-\omega_s t)} . \quad (A2)$$

We expect the radiation from this mechanism to be small. Therefore we are interested in only the dominant (monopole) lowest-order term. Integrating over transverse space to project out this term gives

$$\overline{\mathbf{S}_{\perp 0i}(\bar{z}_i)}=\frac{i8\pi efk_s}{\lambda_s}(\hat{\mathbf{x}}\beta_{x0i}+\hat{\mathbf{y}}\beta_{y0i})e^{-if(k_s z_i-\omega_s t)} , \quad (A3)$$

where the bar denotes the transverse average. Using Eqs. (B8), (9), and (12) this becomes

$$\mathbf{S}_{\perp 0i}(\bar{z}_i)=\frac{i8\pi efk_s}{\lambda_s}[\hat{\mathbf{x}}\beta_{x0i}+\hat{\mathbf{y}}\beta_{y0i}]e^{-if\psi_i}\times\exp\{if[\xi\sin(2k_w\bar{z}_i)+\sigma\sin(k_w\bar{z}_i)+k_w\bar{z}_i]\} , \quad (A4)$$

and with the help of Eq. (29)

$$\overline{\mathbf{S}_{\perp 0i}(\bar{z}_i)}=\frac{i8\pi efk_s}{\lambda_s}e^{-if\psi_i}(\hat{\mathbf{x}}\beta_{x0i}+\hat{\mathbf{y}}\beta_{y0i})\times e^{ifk_w\bar{z}_i}\sum_{n=-\infty}^{\infty}J_n(f\xi)e^{i2nk_w\bar{z}_i}\times\sum_{m=-\infty}^{\infty}J_m(f\sigma)e^{imk_w\bar{z}_i} . \quad (A5)$$

Keeping only nonoscillating terms gives

$$\overline{\mathbf{S}_{\perp 0i}(\bar{z}_i)}=\frac{i8\pi efk_s}{\lambda_s}e^{-if\psi_i}[\hat{\mathbf{x}}\beta_{x0i}+\hat{\mathbf{y}}\beta_{y0i}]\times\sum_{n=-\infty}^{\infty}J_n(f\xi)J_{-(f+2n)}(f\sigma) , \quad (A6)$$

and defining a new drift coupling coefficient

$$\mathcal{H}_f^{\perp}(\xi,\sigma)=2\sum_{n=-\infty}^{\infty} J_n(f\xi)J_{-(f+2n)}(f\sigma) \tag{A7}$$

we have

$$\overline{\mathbf{S}_{\perp 0i}(\bar{z}_i)}=\frac{i4\pi e f k_s a_{wi}}{\lambda_s}\frac{\boldsymbol{\beta}_{\perp 0i}}{a_{wi}/\gamma}\mathcal{H}_f^{\perp}(\xi,\sigma)\frac{e^{-if\psi_i}}{\gamma_i} , \tag{A8}$$

where $\boldsymbol{\beta}_{\perp 0i}=\hat{\mathbf{x}}\beta_{x0i}+\hat{\mathbf{y}}\beta_{y0i}$ is the transverse drift velocity.

Note that the single-electron source in Eq. (A8) is proportional to the ratio of drift velocity to wiggle velocity. Defining the unnormalized emittance for an azimuthally symmetric electron beam as

$$\epsilon=\pi\bar{r}\bar{\beta}_r=\pi k_\beta \bar{r}^2 , \tag{A9}$$

where $k_\beta=a_w k_w/\gamma$ is the betatron wave number,[9] and assuming an electron with $\beta_{\perp 0i}=\bar{\beta}_r$ to be representative of the average electron in the beam, one can write

$$\frac{\boldsymbol{\beta}_{\perp 0i}}{a_{wi}/\gamma}\simeq 2k_w r_e \ll 1 , \tag{A10}$$

where we assumed $\bar{r}=r_e$. Since the electron-beam size is typically much less than the wiggler wavelength, the magnitude of this term for each electron will be small.

An additional comparison should be made between the magnitude of the drift coupling in Eq. (A8) and the dipole of Eq. (61). For dipole coupling to dominate drift coupling we must have

$$\frac{\chi}{2r_e}\mathcal{H}_f^{(2)}(\xi,\sigma)\gg 2k_w r_e \mathcal{H}_f^{\perp}(\xi,\sigma) , \tag{A11}$$

where we approximate the normalized derivative created by the dipole δ functions of Eq. (58) by χ/r_e. Using Eq. (6) this criterion for a single electron becomes

$$\frac{a_w/\gamma}{4(k_w r_e)^2}\gg\frac{\mathcal{H}_f^{\perp}(\xi,\sigma)}{\mathcal{H}_f^{(2)}(\xi,\sigma)} , \tag{A12}$$

where the ratio of the coupling coefficients can be evaluated using Eqs. (34) and (A7). Using Eqs. (B12), (B14), (A9), and (A10), this criterion may be rewritten as

$$\frac{\lambda_s}{2\epsilon}\gg\frac{1}{\xi}\frac{\mathcal{H}_f^{\perp}(\xi,\sigma)}{\mathcal{H}_f^{(2)}(\xi,\sigma)} . \tag{A13}$$

In most cases the dipole source given in Eq. (61) will continue to dominate the drift source of Eq. (A8) even when Eq. (A13) is not satisfied. In modeling the radiation due to an ensemble of electrons (that make up a macroscopic electron beam) the individual electron sources from Eq. (A8) can destructively interfere with one another. If we make the assumption of a matched (constant radius) beam with transverse symmetry, then the resultant drift source from the electron ensemble will be vanishingly small due to the cancellation of electrons with opposite transverse velocities at any specific transverse location. To quantify the magnitude of an electron-beam mismatch, we can define a modulation factor M_f, where $M_f=0$ for a perfectly matched unmodulated beam, and $M_f=1$ for a beam with 100% modulation. Mismatching of the electron beam at the wiggler entrance gives rise to a modulation of the electron beam inside the wiggler. Since the resultant source from the electron ensemble is proportional to M_f, the intensity of the radiation will be proportional to M_f^2. Therefore the drift sources are only important when the inequality in Eq. (A13) is *not* satisfied *and* the factor M_f has order unity. For these cases the source in Eq. (A8) should be added to the sum in Eq. (59).

APPENDIX B

Following Colson,[3] the energy of the ith electron can be given in units of its rest mass as

$$\gamma^{-2}=1-\beta_{\parallel}^2-\beta_{\perp}^2 , \tag{B1}$$

where the i subscripts throughout this derivation have been dropped. From conservation of transverse momentum we know

$$\beta_{\perp}^2=\left[\frac{a_w(x,y,z)}{\gamma}\cos(k_w z)+\beta_{y0}\right]^2+\beta_{x0}^2 , \tag{B2}$$

where the wiggler vector potential is defined

$$a_w(x,y)=\frac{|e|B(x,y)}{mc^2 k_w} , \tag{B3}$$

and β_{x0} and β_{y0} represent electron drift velocities in both transverse directions. Substituting Eq. (B2) in (B1) and solving for $\beta_{\parallel}$ gives

$$\beta_{\parallel}^2=\left\{1-\gamma^{-2}\left[1+\gamma^2\beta_{x0}^2+\gamma^2\left[\frac{a_w(x,y)}{\gamma}\cos(k_w z)+\beta_{y0}\right]^2\right]\right\} , \tag{B4}$$

and assuming $\gamma\gg 1$ and $a_w(x,y)=a_w(x_{0i},y_{0i})=a_w$, we can write

$$\beta_{\parallel}\simeq 1-\frac{1}{2\gamma^2}[1+a_w^2\cos^2(k_w z)+2\gamma\beta_{y0}a_w\cos(k_w z)+\gamma^2\beta_{\perp 0}^2] , \tag{B5}$$

where $\beta_{\perp 0}=(\beta_{x0}^2+\beta_{y0}^2)^{1/2}$ is the transverse drift speed. Note that the electron drift in the x direction does not produce any additional sinusoidal fluctuations in the electron axial velocity as does the drift in the y direction. This is due to the fact that there is no wiggle motion in the x direction. However, this drift must be retained since it modifies the expressions for the ponderomotive phase and the resonance condition.

Averaging Eq. (B5) over a wiggler wavelength we obtain the average axial velocity

$$\bar{\beta}_{\parallel}=1-\frac{1}{2\gamma^2}(1+a_w^2/2+\gamma^2\beta_{\perp 0}^2) , \tag{B6}$$

where γ now represents the average γ over the wiggler period. We use the same symbol here since this difference is negligible for most cases of interest. Using Eqs. (B5) and (B6) we can write

$$\beta_{\parallel}=\bar{\beta}_{\parallel}-\left[\frac{a_w}{2\gamma}\right]^2\cos(2k_w z)-\frac{a_w\beta_{y0}}{\gamma}\cos(k_w z)\ , \tag{B7}$$

and integrating to find the axial position gives

$$z(t)=\bar{z}(t)-\Delta z(t)\ , \tag{B8}$$

where, by judicious choice of the integration constant,

$$\bar{z}(t)=\int_0^t dt\, c\bar{\beta}_{\parallel}=ct\left[1-\frac{1}{2\gamma^2}(1+a_w^2/2)\right] \tag{B9}$$

and

$$\Delta z(t)=\int_0^t dt\left[c\left[\frac{a_w}{2\gamma}\right]^2\cos[2k_w z(t)]+\frac{a_w\beta_{y0}}{\gamma}\cos[k_w z(t)]\right]\ . \tag{B10}$$

To evaluate Δz we keep terms to order $1/\gamma^2$ where we assume $1/\gamma \ll 1$ such that $z(t)$ can be replaced by $\bar{z}(t)$ yielding

$$\Delta z\simeq\left[\frac{a_w}{2\gamma}\right]^2\frac{\sin[2k_w\bar{z}(t)]}{2k_w}+\frac{a_w\beta_{y0}}{\gamma k_w}\sin[k_w\bar{z}(t)]\ . \tag{B11}$$

Using Eqs. (B2) and (B5), and assuming $\gamma \gg 1$, we can solve for the resonance condition including angular effects, given by

$$k_w=\frac{k_s}{2\gamma^2}(1+a_w^2/2+\gamma^2\beta_{\perp 0}^2)\ . \tag{B12}$$

Substituting Eq. (B12) in (B11) gives

$$\Delta z=\frac{\xi}{k_s}\sin[2k_w\bar{z}(t)]+\frac{\sigma}{k_s}\sin[k_w\bar{z}(t)]\ , \tag{B13}$$

where

$$\xi=\frac{a_w^2}{4(1+a_w^2/2+\gamma^2\beta_{\perp 0}^2)} \tag{B14}$$

and

$$\sigma=\frac{2a_w\gamma\beta_{y0}}{1+a_w^2/2+\gamma^2\beta_{\perp 0}^2}\ . \tag{B15}$$

APPENDIX C

To determine how the harmonic radiation is affected by a gradient in the transverse wiggler magnetic field we can take the transverse average of the single-electron source function as was done in Sec. III, but now include a transverse cosh dependence of the wiggler vector potential. The transverse dependence of the wiggler field is given by

$$a_w(x_{0i},y)=a_w(x_{0i})\cosh(k_y y)\ , \tag{C1}$$

and since the electron beam is small with respect to the transverse wiggler wavelength, we can expand the cosh in a power series giving

$$\begin{aligned}a_w(x_{0i},y)&\simeq a_w(x_{0i})[1+k_y^2y^2/2+\cdots]\\&=a_w(x_{0i})[1+k_y^2(\chi_i\sin\theta_r+y_{0i})^2/2+\cdots]\\&=a_w(x_{0i})\left[1+\frac{k_y^2}{2}[y_{0i}^2+2\chi_i y_{0i}\sin\theta_r+\chi_i^2\sin^2\theta_r+\cdots]\right]\\&=a_w(x_{0i})\left[\left[1+\frac{k_y^2y_{0i}^2}{2}\right]+k_y^2\chi_i y_{0i}\sin\theta_r+\cdots\right]\ ,\end{aligned} \tag{C2}$$

where we used Eq. (5) and keep terms to order $O(\chi)$. Note that we have dropped all explicit transverse drift velocity terms for reasons discussed in Appendix A. The term in large parentheses affects only the magnitude of a_w at the electron's guiding center position, and only slightly modifies the amplitude of the source functions in Eqs. (23) and (24). The second term produces a modulation on an optical time scale that induces additional harmonic radiation. This induced even-harmonic emission has the form

$$\begin{Bmatrix}\bar{S}_i^o\\ \bar{S}_i^e\end{Bmatrix}=\frac{i8efk_sk_w}{\lambda_s}e^{-if\psi_i}k_y^2\chi_i y_{0i}\sin\theta_r\times\begin{Bmatrix}\cos\\ i\sin\end{Bmatrix}\{f[\xi\sin(2\theta_r)+\theta_r]\}e^{if\sigma\sin\theta_r}\ , \tag{C3}$$

where we have replaced $a_w(x_{0i},y)$ on Eq. (22) by $a_w(x_{0i},y_{0i})k_y^2\chi_i y_{0i}\sin\theta_r$. In the limit $\sigma\to 0$, this expression gives rise to even-harmonic radiation with even transverse symmetry and odd-harmonic radiation with odd transverse symmetry. In the high-γ regime we typically have $\chi/r_e \ll 1$ so that the radiation caused by the transverse gradient of the wiggler field will be small. Therefore the dominant contribution will be given by the monopole (transverse average) term. This average is given by

$$\begin{aligned}\begin{Bmatrix}\bar{S}_i^o\\ \bar{S}_i^e\end{Bmatrix}&=\frac{i8efk_sk_w}{\lambda_s}e^{-if\psi_i}\int_{-\pi/2}^{\pi/2}d\theta_r\chi_i\frac{\sin(2\theta_r)}{2}k_y^2\chi_i y_{0i}\times\begin{Bmatrix}\cos\\ i\sin\end{Bmatrix}\{f[\xi\sin(2\theta_r)+\theta_r]\}\times\begin{Bmatrix}i\sin\\ \cos\end{Bmatrix}(f\sigma\sin\theta_r)\\&=-\frac{4efk_sk_w}{\lambda_s}k_y^2\chi_i^2y_{0i}e^{-if\psi_i}\int_{-\pi/2}^{\pi/2}d\theta_r\sin(2\theta_r)\times\begin{Bmatrix}\cos\\ \sin\end{Bmatrix}\{f[\xi\sin(2\theta_r)+\theta_r]\}\times\begin{Bmatrix}\sin\\ \cos\end{Bmatrix}(f\sigma\sin\theta_r)\ .\end{aligned} \tag{C4}$$

This integral is identical to the one in Eq. (48) so that

$$\bar{S}_i^e = \frac{i4\pi e f k_s a_w(x_{0i})}{\lambda_s}\left[\frac{i}{2}k_y^2\chi_i y_{0i}\right]\mathcal{K}_f^{(2)}(\xi,\sigma)\frac{e^{-if\psi_i}}{\gamma_i} . \tag{C5}$$

The terms in Eq. (C5) have been grouped so that the term in large parentheses expresses the difference between the harmonic sources due to transverse wiggler field gradients and those due to the transverse gradient in the electron beam [see Eq. (58)]. Note that this term vanishes when the guiding center of the electron approaches the wiggler axis ($y_{0i}\rightarrow 0$). Since this term has a nonzero transverse average, it will radiate primarily as a monopole instead of a dipole pattern as was observed for the electron-beam density gradients in Sec. IV. To get an idea of the magnitude of this radiation source we can look more closely at the term in large parentheses in Eq. (C5) containing the ratio of the electron wiggle amplitude to the transverse wiggler wavelength

$$\left[\frac{i}{2}k_y^2\chi_i y_{0i}\right] \simeq \frac{1}{2}\frac{k_w^2}{2}\frac{a_w}{k_w\gamma}y_{0i} \simeq \frac{a_w k_w r_e}{8\gamma} , \tag{C6}$$

where we assumed $y_{0i}\simeq r_e/2$.

The even-harmonic term in Eq. (58) of Sec. V contains a difference of δ functions which scale like

$$\tfrac{1}{2}[\delta(y-y_{0i}-\chi/2)-\delta(y-y_{0i}+\chi/2)] \rightarrow \frac{\chi}{2r_e}\simeq\frac{a_w}{2\gamma k_w r_e} . \tag{C7}$$

Since the harmonic power scales roughly like the coupling coefficient squared, the radiation caused by gradients in the wiggler field will be $[\lambda_w/(\pi r_e)]^4$ times weaker than the radiation caused by gradients in the electron-beam density. This is what one would intuitively expect since the wiggler field gradient caused by the large separation of the wiggler magnets is much smaller than the density gradient inside the narrow electron beam.

APPENDIX D

The multipole coupling due to the mth derivative of the electron density can be evaluated as follows. Each term in Eq. (40) is given by

$$\mathcal{S}_{m+1} = C\int_{y-\chi_i}^{y+\chi_i}\begin{Bmatrix}\cos\\ i\sin\end{Bmatrix}\{f[\xi\sin(2\theta_r)+\theta_r]\}\times\frac{(y_{0i}-y)^m}{m!}e^{if\sigma\sin\theta_r}n^{(m)}(y)dy_{0i} , \tag{D1}$$

where (m) superscript denotes the mth derivative with respect to y and C is defined in Eq. (42). Using Eq. (5) (without the drift term) this becomes

$$\mathcal{S}_{m+1} = -i\frac{(-1)^m n^{(m)}(y)\chi^{m+1}}{m!}\times C\int_{-\pi/2}^{\pi/2}\begin{Bmatrix}\cos\\ i\sin\end{Bmatrix}\{f[\xi\sin(2\theta_r)+\theta_r]\}\times\sin^m\theta_r\cos\theta_r e^{if\sigma\sin\theta_r}d\theta_r . \tag{D2}$$

For $m=2$ (the tripole term) we have

$$\mathcal{S}_3 = \frac{n''(y)\chi^3}{2}C\int_{-\pi/2}^{\pi/2}\begin{Bmatrix}\cos\\ i\sin\end{Bmatrix}\{f[\xi\sin(2\theta_r)+\theta_r]\}\times\tfrac{1}{4}[\cos\theta_r-\cos(3\theta_r)]\times e^{if\sigma\sin\theta_r}d\theta_r . \tag{D3}$$

Evaluating the integrals as before yields

$$\mathcal{S}_3 = -\frac{n''(y)C\chi^3\pi}{16}[\mathcal{K}_f^{(1)}(\xi,\sigma)-\mathcal{K}_f^{(3)}(\xi,\sigma)] . \tag{D4}$$

To model this effect we assume a discrete tripole of the form

$$S_3^\dagger(y) = W_3\{\delta(y-y_{0i})-\tfrac{1}{2}[\delta(y-y_{0i}+\chi/2)+\delta(y-y_{0i}-\chi/2)]\} \tag{D5}$$

so that, using Eq. (46), the discrete resultant source for the third term in the Taylor series expansion of the density is given by

$$\begin{aligned}\mathcal{S}_3^\dagger(y) &= \int_{y-\chi_i}^{y+\chi_i} W_3\{\delta(y-y_{0i})-\tfrac{1}{2}[\delta(y-y_{0i}+\chi/2)+\delta(y-y_{0i}-\chi/2)]\}n(y_{0i})dy_{0i}\\ &= W_3\{n(y)-\tfrac{1}{2}[n(y-\chi/2)+n(y+\chi/2)]\}\\ &= W_3\left\{n(y)-\frac{1}{2}\left[\left[n(y)-\frac{\chi}{2}n'(y)+\frac{\chi^2}{8}n''(y)-\cdots\right]+\left[n(y)+\frac{\chi}{2}n'(y)+\frac{\chi^2}{8}n''(y)+\cdots\right]\right]\right\}\\ &= W_3\left[n(y)-\frac{1}{2}\left[2n(y)+\frac{\chi^2}{4}n''(y)-\cdots\right]\right] ,\end{aligned} \tag{D6}$$

and keeping only the lowest-order term gives

$$\mathcal{S}_3^\dagger(y) = \frac{W_3\chi^2 n''(y)}{8} . \tag{D7}$$

Solving for W_3 by equating Eqs. (D4) and (D7) gives

$$W_3 = -\frac{\pi}{2} C\chi[\mathcal{H}_f^{(1)}(\xi,\sigma) - \mathcal{H}_f^{(3)}(\xi,\sigma)] , \tag{D8}$$

so that the discrete single-electron source given in Eq. (D5) becomes

$$S_3^{\dagger}(y) = -\frac{\pi}{2} C\chi[\mathcal{H}_f^{(1)}(\xi,\sigma) - \mathcal{H}_f^{(3)}(\xi,\sigma)]\{\delta(y - y_{0i}) - \tfrac{1}{2}[\delta(y - y_{0i} - \chi/2) + \delta(y - y_{0i} + \chi/2)]\} .$$

Higher-order multipoles can be obtained through similar analysis. However, for slowly varying density distributions, the higher multipoles will not have a significant contribution due to their dependence on the higher-order derivatives of $n(y_{0i})$.

[1]W. B. Colson, IEEE J. Quantum Electron. **QE-17**, 1417 (1981).

[2]J. M. J. Madey and R. C. Taber, in *Physics of Quantum Electronics,* edited by Jacobs *et al.* (Addison-Wesley, Reading, MA, 1980), Vol. 7, Chap. 30.

[3]W. B. Colson, G. Dattoli, and F. Ciocci, Phys. Rev. A **31**, 828 (1985).

[4]W. Becker, Z. Phys. B **42**, 87 (1981).

[5]W. Becker, Z. Phys. D **7**, 353 (1988).

[6]The paraxial wave equation invokes the slowly varying envelope approximation as discussed in Ref. 7. The analogous expression for a Hermite Gaussian mode set is derived in Ref. 8.

[7]M. Sargent, M. O. Scully, and W. E. Lamb, *Laser Physics* (Addison Wesley, Reading, MA, 1974), p. 100.

[8]M. J. Schmitt and C. J. Elliott, Phys. Rev. A **34**, 4843 (1986).

[9]E. T. Scharlemann, J. Appl. Phys. **58**, 2154 (1985).

[10]W. M. Sharp, E. T. Scharlemann, and W. M. Fawley, *Proceedings of the Eleventh International Conference on Free Electron Lasers, Naples, FL, 1989,* edited by L. R. Elias and I. Kimel (North-Holland, Amsterdam, in press).

[11]*Table of Integrals, Series, and Products,* edited by I. S. Gradshteyn and I. M. Ryzhik (Academic, New York 1980), Eqs. 8.411.2,3.

[12]C. Leubner, Phys. Rev. A **23**, 2877 (1981).

[13]B. D. McVey, Nucl. Instrum. Methods A **250**, 449 (1986).

[14]D. J. Bamford and D. A. G. Deacon, Phys. Rev. Lett. **62**, 1106 (1989).

[15]M. J. Schmitt and C. J. Elliott, in *Proceedings of the Eleventh International Conference on Free Electron Lasers* (Ref. 10).